On ozone-photocatalysis synergism in black-light induced reactions: oxidizing species production in photocatalytic ozonation versus heterogeneous photocatalysis

E. Mena[1], A. Rey [1]*, B. Acedo[1], F. J. Beltrán[1], S. Malato[2]

[1]Departamento de Ingeniería Química y Química Física, Facultad de Ciencias, Universidad de Extremadura, 06006 Badajoz, Spain

[2]Plataforma Solar de Almería (CIEMAT), Carretera Senés km 4, 04200 Tabernas (Almería), Spain

Abstract

The synergism produced between ozone and TiO_2 black light photocatalytic oxidation of methanol has been studied following the rate of formaldehyde formation during photocatalytic oxidation, ozonation and photocatalytic ozonation experiments. Methanol was selected as a model compound due to its low reaction rate with molecular ozone and its scavenging character for both, free hydroxyl radicals and trapped holes. TiO_2-P25 was used as photocatalyst and black light blue lamps (emitting with a maximum at 365 nm) as radiation source. The effect of ozone concentration and pH was evaluated. Absorbed light intensity by the photocatalyst was also determined to calculate the quantum yields of photocatalytic reactions. Three main processes need to be considered during photocatalytic ozonation: direct ozone-methanol reaction, indirect ozone reactions and photocatalytic reactions, which allow calculating the quantum yield of photo-generated oxidizing species. The presence of ozone exerts a positive effect in the reaction rate of oxidizing species formation due to light induced reactions also enhancing the quantum yield from 0.34 to 0.80 mol·einstein^{-1} at pH=3 (where indirect ozone reactions are negligible). This parameter increased from 0.29 to 3.27 mol·einstein^{-1} at pH=7 likely due to indirect ozone reactions that cannot be disregarded. The positive effect of ozone in the photocatalytic induced reactions has been attributed to the reaction of dissolved ozone and hydrogen peroxide (formed upon methanol direct ozonation) as electron acceptors, thus reducing the recombination process on the catalyst surface to some extent. A simplified economic study is also presented.

Keywords

Photocatalytic ozonation, ozone, TiO_2, synergism, methanol, formaldehyde

1. Introduction

Wastewater is one of the most important problems in industrialized regions. Many of these effluents contain high concentrations of organic pollutants that must be removed in order to fulfill the required limits of the increasingly restrictive legislation. In this context, photocatalytic detoxification treatments based on TiO_2 semiconductor have been the focus of numerous investigations in the last 30 years for the destruction of undesirable contaminants in water [1,2,3]. In heterogeneous photocatalysis, photoinduced holes and electrons in semiconductor particles, through a complex reaction mechanism, give place to highly oxidizing species which play a key role in degradation of organic pollutants. The most commonly used semiconductor has been polycrystalline powders of titanium dioxide due to unique properties such as chemical stability, safety and low cost [2]. However, its photohole-electron recombination is a serious problem for the development of photocatalytically based technologies since it severely limits the quantum yields achievable [2,3,4]. Several strategies have been proposed to minimize this problem and increase the process efficiency (ion doping, different semiconductors coupling, using chemical oxidants or combining photocatalysis with other Advanced Oxidation Processes (AOPs) [2]). Among them, the combination of ozone and heterogeneous photocatalysis with TiO_2 (photocatalytic ozonation) has demonstrated to be an efficient treatment enhancing the formation of oxidizing species compared to the single ozonation or photocatalytic processes [5,6].

When a semiconductor (e.g. TiO_2) is irradiated with a photon of energy greater than its band gap energy an electron/hole pair is formed in the conduction band (CB) and valence band (VB), respectively. These mobile species can migrate to the TiO_2 surface and/or can be readily trapped forming less mobile states (to simplify e^-/h^+ stand for all the forms of holes and electrons).

$$TiO_2 + h\nu \rightarrow e^- + h^+ \quad (1)$$

In addition, these species can give place to the recombination reaction (2):

$$e^- + h^+ \rightarrow TiO_2 \quad (2)$$

The nature of trapped holes has been controversially discussed [7,8]. It has been generally assumed that adsorbed water could be photooxidized giving place to surface bounded hydroxyl radicals ($^{\bullet}OH_s$). However, it has been reported that this reaction was kinetic and thermodynamically hindered [7] and the trapping phenomena by terminal oxygen ions of the

TiO_2 lattice (O^{2-}_{TiO2}) has been proposed, forming terminal protonated or deprotonated radicals (depending on pH) [9,10]. Regardless the reaction considered, the formation of hydroxyl radicals in the TiO_2 surface can be described:

$$h^+ \xrightarrow{H_2O/O^{2-}TiO_2} {}^{\bullet}OH_s \ ({}^{\bullet}O_s^-) \quad (3)$$

In addition, oxygen when present on the particle surface, acts as an electron acceptor according to reaction (4):

$$e^- + O_2 \rightarrow O_2^{\bullet -} \quad (4)$$

Superoxide ion radicals ($O_2^{\bullet -}$) may give place to hydrogen peroxide that can react with TiO_2 electrons and/or additional $O_2^{\bullet -}$, forming free hydroxyl radicals through reactions (5) to (6):

$$O_2^{\bullet -} + O_2^{\bullet -} + 2H^+ \rightarrow H_2O_2 + O_2 \quad (5)$$

$$e^- \ (O_2^{\bullet -}) + H_2O_2 \rightarrow {}^{\bullet}OH + OH^- (+O_2) \quad (6)$$

In this complex (but simplified) reaction mechanism, free hydroxyl radicals, $^{\bullet}OH$, and/or trapped holes (h^+ = $^{\bullet}OH_s$/$^{\bullet}O_s^-$), may be responsible of the non-selectively organic matter oxidation and mineralization (reaction (7)), being this process among the most studied AOPs.

$${}^{\bullet}OH(h^+) + R \rightarrow R' + {}^{\bullet}OH(h^+) \rightarrow [...] \rightarrow CO_2 + H_2O \quad (7)$$

When ozone is present, it can react directly and selectively with some organic compounds (i.e. aromatic and substituted aromatic compounds, molecules with unsaturated bonds e.g. -C=C-, -C≡C-, -C=N, -C=O, etc) through different reaction mechanisms (mainly cycloaddition reactions and/or electrophilic substitution) included in “direct ozone reactions” terminology (reaction (8)) [11].

$$zO_3 + R \rightarrow R'(+H_2O_2) \quad (8)$$

On the other hand, the presence of radical species (i.e. mainly $^{\bullet}OH$) coming from the decomposition of ozone in water gives place to the non-selectively oxidation of the organic compounds in water (indirect ozone reactions), process that is favored in alkaline media [11]:

$$O_3 + OH^- \rightarrow HO_2^- + O_2 \quad (9)$$

$$O_3 + HO_2^- \rightarrow HO_2^\bullet + O_3^{\bullet-} \quad (10)$$

$$HO_2^\bullet \xrightleftharpoons{pK=4.8} O_2^{\bullet-} + H^+ \quad (11)$$

$$O_3 + O_2^{\bullet-} \rightarrow O_3^{\bullet-} + O_2 \quad (12)$$

The generated ozonide radical ($O_3^{\bullet-}$) rapidly reacts with H^+ in the solution to give $HO_3^\bullet$ radical, which evolves to give O_2 and $^\bullet OH$ (reactions (13) and (14)).

$$O_3^{\bullet-} + H^+ \rightarrow HO_3^\bullet \quad (13)$$

$$HO_3^\bullet \rightarrow {}^\bullet OH + O_2 \quad (14)$$

The benefits of using the combined process, photocatalytic ozonation, are not only related to the sum of individual processes but also to the fact that the dissolved ozone can readily react with electrons at the TiO_2 surface according to reaction (15) giving place to the ozonide ion radical:

$$O_3 + e^- \rightarrow O_3^{\bullet-} \quad (15)$$

As a consequence, the recombination of electrons and positive holes may be reduced by this reaction (15) and also by reaction (6) due to the presence of higher H_2O_2 concentration in the reaction medium, eventually formed during direct ozonation reactions (reaction (8)) [12,13,14]. With this reaction scheme a synergistic effect between ozone and semiconductor photocatalysis is expected due to the larger amount of oxidizing species formed (hydroxyl radicals, bounded hydroxyl radicals and/or positive holes). This has been observed for the photocatalytic ozonation of several organic compounds in water [2,5,6,15,16,17,18,19].

Some of the target compounds subjected to photocatalytic ozonation were complex molecules that present high direct ozone-organic rate constants and/or also complicated reaction pathways involving several steps with different intermediate species [5,16,19]. This makes difficult to analyze the reaction mechanism, the species involved in the oxidation steps and/or the synergistic effect between ozone and photocatalysis. In that sense, it would be interesting to test the photocatalytic ozonation process using small and refractory organic compounds to direct ozone reactions.

In this work methanol has been selected due to its known scavenging character of hydroxyl radicals (k_{OH}=9.7x10^8 $M^{-1}s^{-1}$, [20]) and that also has been commonly used to test the photocatalytic efficiency of several TiO_2 materials since it reacts with photogenerated holes [9,10,21,22,23,24,25]. In addition, methanol-ozone direct reaction takes place at slow reaction rate (k_{O3}=0.024 $M^{-1}s^{-1}$) [26]. Therefore, it is expected that under appropriate experimental conditions, the formaldehyde evolution (formaldehyde is the first product of methanol oxidation) gives information about the production rate of oxidizing species (different from O_3). The aim of this work was then to evaluate the production of photo-generated oxidizing species (hydroxyl radicals and positive holes) using methanol as target compound comparing both, photocatalytic oxidation and photocatalytic ozonation, to determine the true quantum yield of photocatalytic reactions, and to state the synergy degree between ozone and irradiated semiconductor during photocatalytic ozonation. To our knowledge the determination of the quantum yield of photo-generated oxidizing species production in photocatalytic ozonation has not been studied before with any target compound.

2. Experimental section

2.1. Experimental set-up and oxidation/ozonation procedure

Ozonation, photocatalytic oxidation and photocatalytic ozonation experiments were carried out in a 1L slurry cylindrical reactor equipped with magnetic stirring and inlets for measuring temperature, feeding the gas (oxygen or ozone-oxygen) through a porous plate situated at the reactor bottom, sampling port and outlet for the non-absorbed gas. In photocatalytic experiments, the reactor was illuminated with 2 black light blue (UVA radiation) fluorescent lamps (15 W each, from HQPower) placed inside a black box.

The reactor was charged with an aqueous solution containing methanol (2 M, CH_3OH HPLC grade from Panreac) and TiO_2 (0.5 gL^{-1}, Degussa P25, in catalytic experiments). Initial pH was set to 3 with $HClO_4$, pH=7 with NaOH or buffered at pH=7 with H_3PO_4 (30 mM) and NaOH (from Panreac). In photocatalytic experiments, the reactor was then exposed to the radiation (lamps were turned on 30 min before to stabilize). In ozonation experiments a mixture of ozone-oxygen gas (30 Lh^{-1}, 10-30 mgL^{-1}) was also continuously fed to the reactor. Ozone was generated from pure oxygen in a Sander laboratory ozonator. Temperature was maintained at 25º C during the reaction time. Reaction samples were withdrawn from the reactor at regular intervals for 60 min reaction time, and then filtered through syringe PET membrane filters (Chromafil Xtra, 0.20 µm). The evolution of the reaction was followed through the determination of formaldehyde (primary product of methanol oxidation),

hydrogen peroxide, dissolved ozone concentration, ozone concentration in the outlet gas and pH.

Formaldehyde was determined by the Nash method [27], based on the Hantzsch reaction. In this assay, 2 mL of reagent (0.2 mL of acetylacetone (Sigma-Aldrich), 3 mL of acetic acid (Panreac) and 25 g of ammonium acetate (Fluka) in 100 mL of water) are mixed with 5 mL of the sample, heated for 30 min at 50º C in the dark [28]. Spectrophotometric measurements were carried out at 412 nm (ε=7890 $M^{-1}cm^{-1}$) using a Helios-α Thermo Spectronic spectrophotometer. Hydrogen peroxide concentration was determined through the cobalt/bicarbonate method [29], at 260 nm (ε=26645 $M^{-1}cm^{-1}$) using a Helios-α spectrophotometer. Dissolved ozone concentration was measured by following the method proposed by Bader and Hoigné [30] based on the decoloration of a 5,5,7 indigotrisulphonate solution (λ=600 nm, Helios-α spectrophotometer, ε=20000 $M^{-1}cm^{-1}$). Ozone in the gas phase was monitored by means of an Anseros Ozomat ozone analyzer, based on the absorbance at 254 nm.

2.2. Photon fluxes determination

Ferrioxalate actinometry [31] was used to determine the incident photon flux, I_0, in the photoreactor, that was found to be $2.66x10^{-5}$ einstein·min^{-1}. In these experiments the Fe(II) concentration was followed by the o-fenantroline method [32] using a Helios-α spectrophotometer at 510 nm (ε=11023 $M^{-1}cm^{-1}$). The photon flux, I_a, absorbed by the catalyst was estimated through the determination of the quantum yield of formaldehyde generation in the photoreactor. This was obtained by applying the protocol of Serpone and Salinaro [33] for the photocatalytic oxidation of methanol, analyzing the formaldehyde evolution under the following operating conditions: methanol concentration from 0.5 to 2 M, TiO_2 concentration from 0.025 to 3 g·L^{-1}, pH_0=7, pH=7 (buffered) and pH_0=3 (adjusted with NaOH, phosphate buffered or adjusted with $HClO_4$, respectively) and oxygen saturated solution with 30 L·h^{-1} gas flow rate. The evolution of the reaction was followed as explained in the previous section. For comparative purposes, additional photocatalytic oxidation experiments were carried out using formic acid 0.01 M as target compound (0.5 gL^{-1} TiO_2, pH_0=3). Formic acid was determined following the evolution of the CO_2 formed by measuring the total organic carbon (TOC) remaining in the solution using a TOC-V_{SCH} analyzer from Shimadzu.

3. Results and discussion

3.1. Absorbed photon flux

The determination of the absorbed photon flux by the catalyst is a key issue in heterogeneous photocatalytic reactions that serves to calculate the quantum yield of the reaction according to equation (16):

$$\varphi_i = \frac{reacted\ molecules}{absorbed\ photons} = \frac{r_i}{I_a} \quad \left(\frac{mol\ i}{einstein}\right) \tag{16}$$

The radiant energy used in a photocatalytic reaction (absorbed, I_a) is generally lower than that impinging on the reacting system (I_0) due to the light scattered or reflected by the suspended catalyst in the dispersion. The absorbed light intensity has been usually calculated by applying the radiation transfer equation (RTE) to the reaction system [34,35,36,37,38] or experimentally determined by means of the measurement of the light transmission through a photocatalyst suspension [39].

In this work, we have indirectly calculated the absorbed photon flow by using the protocol of Serpone and Salinaro [33] to determine the quantum yield of the methanol oxidation reaction (formaldehyde formation) under our experimental conditions.

Methanol photocatalytic oxidation gives place to formaldehyde as primary oxidation product according to reactions (17) and (18):

$$CH_3OH + h_T^+ (^\bullet OH) \rightarrow {}^\bullet CH_2OH + H^+ (H_2O) \tag{17}$$

$$^\bullet CH_2OH + O_2 \rightarrow {}^\bullet O_2CH_2OH \rightarrow CHOH + H^+ + O_2^{\bullet -} (HO_2^\bullet) \tag{18}$$

where either holes (h^+) and free hydroxyl radicals ($^\bullet$OH) may participate, forming also superoxide ion radical ($O_2^{\bullet -}$) or hydroperoxide radical (acidic pH) ($HO^\bullet_2$). Fig.1 shows the time-evolution of CHOH formation under different experimental conditions. It was nearly linear throughout the range of conditions used. The rate of CHOH formation reached a plateau around 2 M methanol, as can be seen in Fig.2. This concentration was then used for the experiments with different TiO_2 concentration. At this CH_3OH concentration, formaldehyde is not expected to be significantly oxidized since oxidizing species will mainly react with the former. In fact, taking into account the kinetic constants of methanol and formaldehyde with hydroxyl radicals (9.7×10^8 and 1×10^9 $M^{-1}s^{-1}$ [20], respectively) the formaldehyde formation rate with 2 M methanol was 1940 times higher than formaldehyde oxidation rate (using a generic concentration about 10^{-3} M similar to CHOH concentrations observed in this work) proving that formaldehyde oxidation could be negligible in the overall reaction rate. The calculated reaction rates of formaldehyde formation at different TiO_2

loading defines a plateau from 0.5 g·L^{-1} as depicted in Fig. 3A. This behavior can be well described through the equation (19):

$$\xi = \frac{\xi_{\lim} a C_{TiO2}}{\xi_{\lim} + a C_{TiO2}} = \frac{r_{CHOH}}{I_0} \quad (19)$$

where photonic efficiencies are calculated employing the relationship $\xi = r_{CHOH}/I_0$. The quantum yield of formaldehyde formation (φ_{CHOH}) was determined from the limiting photonic efficiency ($\xi_{\lim}$) at high TiO_2 loadings. At these conditions it has been reported that $\xi_{\lim} = \varphi$ [33]. Fig.3B shows fitting results of linearized equation (19). The quantum yield calculated for formaldehyde formation at pH_0=7 (non-buffered) was $\varphi_{CHOH-pH7}$ =0.48 mol·einstein^{-1}. The pH value did not change significantly (pH_f=6.7). The corresponding absorbed light intensity at different TiO_2 loadings are summarized in Table 1 together to the integrated absorption fraction over the wavelength used here, $F_s = I_a/I_0$. From 0.5 g·L^{-1} TiO_2 onward, the P25 catalyst presented an absorption fraction higher than 90%. On the other hand, in experiments carried out at pH=7 (phosphate buffered solution), the reaction rate of formaldehyde formation was lower than in the previous case at the same operating conditions (catalyst loading, methanol concentration) as can also be observed in Fig.1 and Table 1. This can be due to phosphate adsorption onto the titania surface [40,41], that can compete for adsorption sites with methanol and/or react with oxidizing species formed at the catalyst surface (e.g. with hydroxyl radicals, $k_{OH\text{-}PO4^{3-}}$=1x10^7 M^{-1}s^{-1}, $k_{OH\text{-}HPO4^{2-}}$=1.5x10^5 M^{-1}s^{-1}, $k_{OH\text{-}H2PO4^{-}}$=2x10^4 M^{-1}s^{-1}, $k_{OH\text{-}H3PO4}$=2.7x10^6 M^{-1}s^{-1} [20]), although this second point could be disregarded due to the great excess of methanol (2 M CH_3OH against 30 mM H_3PO_4). Since phosphates do not absorb the black light used, it is expected that the absorbed light intensity, I_a, do not change significantly compared to the non-buffered experiments at pH=7.

On the other hand, it is known that the size of the TiO_2 aggregates in aqueous solution depends on the pH value and therefore, could affect the intensity of light absorbed by the photocatalyst [2]. Thus, additional photocatalytic oxidation experiments with 0.025-1 g·L^{-1} TiO_2 were carried out at pH_0=3 to calculate both, the quantum yield ($\varphi_{CHOH-pH3}$) and the absorbed photon flow at this pH value. Firstly, the pH value did not significantly change during the reaction time. It was observed that the rate of formaldehyde formation at pH_0=3 was quite lower than at pH_0=7 (non-buffered) at the same catalyst loading (see Fig.1). These results have also been plotted in Fig.3A whereas Fig.3B shows fitting results of linearized equation (19) for experiments at pH_0=3. The quantum yield calculated was $\varphi_{CHOH-pH3}$=0.34 mol·einstein^{-1}. The absorbed light intensity calculated was somewhat higher than at pH=7 in

experiments at the same catalyst loading (Table 1), according to the lower aggregates size expected at lower pH. The lower reaction rates and quantum yield observed could be attributed to the stabilization of the $^{\bullet}O_2CH_2OH$ radical at acidic pH [42] and/or to the presence of ClO_4^- ions ($HClO_4$ used to set pH=3) that can be absorbed onto the catalyst surface [43]. Previously, Du and Rabani [42] showed that quantum yields of formaldehyde formation during photocatalytic oxidation of methanol with a TiO_2 catalyst fell down from 0.2 to 0.05 mol·einstein^{-1} at pH=7 and pH=3, respectively, whereas when comparing the quantum yield of CO_2 formation during photocatalytic oxidation of formic acid at pH=3, the value was quite similar to that found for the methanol system at pH=7. This was explained on the basis of the stabilization of the $^{\bullet}O_2CH_2OH$ radical at acidic pH when using methanol. However, our experiments carried out at pH=3 with formic acid 0.01 M (high enough to reach constant reaction rate independent of formic acid concentration [42]) led to the results summarized in Table 1, where the photonic efficiency calculated for CO_2 formation was 0.26 mol·einstein^{-1}, quite similar (even lower) than the value obtained in the methanol system. These results seem to be pointed out that the stabilization of the $^{\bullet}O_2CH_2OH$ radical at pH=3 is not the main responsible of the decrease observed in the quantum yield at this pH value under the operating conditions used here and, therefore, we have used also methanol at pH=3 as model compound.

Finally, under the same experimental conditions, I_a is not expected to significantly change in presence of ozone during photocatalytic ozonation experiments since O_3 does not absorb black light radiation (λ=365 nm). The calculated I_a values were used to determine the quantum yields for photocatalytic ozonation processes for comparative purposes.

3.2. Photocatalytic oxidation versus photocatalytic ozonation

To compare photocatalytic oxidation behavior versus photocatalytic ozonation, similar experiments were carried out at the same operating conditions of methanol concentration, gas flow rate, radiation and pH, but feeding ozone to the system. At 2 M methanol concentration used here, also in ozonation and photocatalytic ozonation experiments, formaldehyde ozonation is not expected. According to the kinetic constants of methanol and formaldehyde with O_3 (0.024 and 0.10 $M^{-1}s^{-1}$ [26], respectively) and the concentration of both compounds, the formaldehyde formation rate with 2 M methanol was almost 500 times higher than the formaldehyde ozonation (using a generic concentration about 10^{-3} M similar to CHOH concentrations observed in this work) proving that formaldehyde ozonation could be neglected in the overall reaction rate.

The comparison of formaldehyde formation during photocatalytic oxidation (TiO_2/O_2/UVA) and photocatalytic ozonation (TiO_2/O_3/UVA) of methanol is presented in Fig.4A. Also, for

comparative purposes single ozonation (O_3) and photolytic ozonation results (i.e. irradiated O_3 without TiO_2, O_3/UVA) have been plotted. These experiments were carried out at pH=3 to minimize indirect ozone reactions. This pH value did not significantly change throughout the reaction time. As expected, ozonation and photolytic ozonation gave place to similar formaldehyde evolution since ozone does not absorb black light radiation. On the other hand, the results observed for photocatalytic oxidation are also quite similar to the ozone process. The highest rate of formaldehyde formation was found during photocatalytic ozonation. Reaction rates were calculated through the slope of the CHOH concentration-time evolution and are displayed in Table 2. A synergistic effect between ozone and the irradiated TiO_2 can be observed during TiO_2/O_3/UVA treatment where the reaction rate is almost twice higher than the sum of the reaction rates of individual process ($2.91x10^{-5}$ $M \cdot min^{-1}$ vs. $1.89x10^{-5}$ $M \cdot min^{-1}$, respectively).

The accumulation of important concentrations of hydrogen peroxide was also observed during ozonation experiments. Results are plotted in Fig.4B. As can be seen, during photocatalytic oxidation of methanol small amounts of hydrogen peroxide could be detected whereas during single ozonation and photolytic ozonation, the evolution of hydrogen peroxide is comparable to the formaldehyde formation. This is explained on the basis of ozone-methanol direct reaction which gives place to hydrogen peroxide [44] according to:

$$O_3 + CH_3OH \rightarrow CHOH + H_2O_2 \quad (20)$$

It is noticeable that hydrogen peroxide concentration was much lower in the photocatalytic ozonation experiment likely due to the consumption of H_2O_2 through reaction (6) (H_2O_2-e_{aq}^- reaction: $k=1.1x10^{10}$ $M^{-1}s^{-1}$ [20]). This reaction will also enhance the generation of hydroxyl radicals improving methanol oxidation.

In addition, dissolved ozone was measured during all the ozonation experiments. The concentration was nearly constant at $7.5x10^{-6}$ M and $4.5x10^{-6}$ M during ozonation and photocatalytic ozonation, respectively. Also the ozone concentration in the gas phase in the reactor outlet was lower during photocatalytic ozonation (5.0 mgL^{-1}) than during ozonation (6.5 mgL^{-1}). The lower values found during photocatalytic ozonation suggests that O_3 is also been consumed through reaction (15) (O_3-e_{aq}^- reaction: $k=3.6x10^{10}$ $M^{-1}s^{-1}$, which is also higher than the one of O_2-e_{aq}^- reaction: $k=1.9x10^{10}$ $M^{-1}s^{-1}$ [20]), improving methanol oxidation rate due to the generation of additional hydroxyl radicals.

Therefore, taking into account the slow reaction rate of direct methanol ozonation and the negligible contribution of ozone decomposition at the pH value used here, the synergism observed may be related to the reaction of dissolved ozone and hydrogen peroxide as

electron acceptors to produce •OH radicals, thus avoiding in some extent the recombination reactions on the TiO_2 catalyst.

3.2.1. Influence of ozone concentration

The influence of ozone concentration in the feeding gas during photocatalytic ozonation of methanol was studied at pH=3. Results of formaldehyde and hydrogen peroxide formation with time are depicted in Fig.5A and Fig.5B, respectively. Also, for the sake of comparison, single ozonation results varying the ozone gas concentration have been plotted. It can be observed that ozone concentration exerts a positive effect on the methanol oxidation rate (formaldehyde formation), compared to the ozone free experiments (see also Fig.4A) both in single ozonation and photocatalytic ozonation, although the effect is less important when increasing the ozone gas concentration. Reaction rates of formaldehyde formation have been calculated and are shown in Table 2. The increase of formaldehyde formation rate is proportional to the increasing ozone concentration in single ozonation experiments whereas it is more important from 10 to 20 mgL^{-1} of ozone than from 20 to 30 mgL^{-1} in photocatalytic ozonation. This behavior has been observed before during photocatalytic ozonation process [19] and has been attributed to complex Langmuir kinetics for substances that absorb and react on the semiconductor surface.

Regarding the evolution of H_2O_2 during the experiments at different O_3 concentration (Fig.5B), it can be observed that H_2O_2, formed mainly from direct ozonation of methanol, is further accumulated during ozonation treatment while is not in the photocatalytic ozonation process and regardless of the ozone concentration. The latter is likely due to the consumption of H_2O_2 in the photocatalytic process through reaction (6). Despite this, a positive effect of ozone concentration is observed on the evolution of H_2O_2 in both treatments, more pronounced during ozonation.

3.2.2. Influence of pH

Previous experiments have been carried out at pH=3 to minimize ozone decomposition reaction and, thus, avoiding indirect methanol-ozone oxidation reaction. However, pH plays a crucial role during ozonation processes. Results of photocatalytic oxidation, ozonation and photocatalytic ozonation of CH_3OH at pH=3 and pH=7 (buffered solution) are compared in Fig.6. Regarding CHOH formation, slight differences were observed in Fig.6A for photocatalytic oxidation reaction at pH=3 and pH=7 as commented in the previous section. Nevertheless, when ozone is present, a large increase in the rate of CHOH formation is observed at pH=7 respect to pH=3. During single ozonation experiments the formaldehyde formation rate increased around 8 times (from $1.97x10^{-5}$ to $1.55x10^{-4}$ $M \cdot min^{-1}$, see Table 2).

Direct ozone-methanol reaction is not affected by pH modifications since CH_3OH does not dissociate at the studied pH range [26]; as a consequence, this behavior is related to ozone decomposition reactions (9)-(14) that are produced at neutral pH to generate $^{\bullet}OH$ radicals in the reaction medium. In this line, lower dissolved ozone concentration has been detected at pH=7 ($8x10^{-7}$ M and $1x10^{-6}$ M in ozonation and photocatalytic ozonation, respectively) compared to pH=3 ($8.2x10^{-6}$ M and $6.1x10^{-6}$ M in ozonation and photocatalytic ozonation, respectively). Also, ozone concentration in the gas phase at the reactor outlet has been observed to decrease with pH increase from 3 to 7 (from 15 at pH 3 to 10 mgL^{-1} at pH 7 in ozonation, and from 11 at pH 3 to 6 mgL^{-1} at pH 7 in photocatalytic ozonation runs). This corroborates a higher consumption of ozone at neutral pH likely due to its faster decomposition.

In addition, hydrogen peroxide formed upon direct ozone-methanol reaction can be dissociated (reaction (21), pK=11.3), promoting reaction (10) to some extent:

$$H_2O_2 \xrightleftharpoons{pK=11.3} HO_2^- + H^+ \quad (21)$$

In fact, hydrogen peroxide concentrations detected at pH=7 were fairly lower than at pH=3 (see Fig.6B), indicating that H_2O_2 is consumed during the single ozonation process. Another fact that can affect the ozonation mechanism due to the pH value is that the hydroperoxil radical formed upon methanol-$^{\bullet}OH$ oxidation ($HO_2^{\bullet}$) will be on its dissociated form ($O_2^{\bullet-}$) at neutral pH (reaction (11), pK=4.8), then it also participates in the reaction mechanism of ozone decomposition.

The increase of formaldehyde formation rate observed was more significant in photocatalytic ozonation due to the formation of higher concentration of oxidizing species at the photocatalyst surface according to the reaction scheme described above. At pH=7 and 30 mgL^{-1} of ozone inlet concentration, the synergistic effect is clearly observed in the reaction rate at this pH value (see Table 2), where the sum of ozone and photocatalytic oxidation rates was $1.62x10^{-4}$ $Mmin^{-1}$ fairly lower than that of photocatalytic ozonation ($2.38x10^{-4}$ $Mmin^{-1}$). Therefore, an increment in the pH value exerts a positive effect on the photocatalytic ozonation reaction due to the formation of species that favor the ozone decomposition in water.

3.2.3. Synergistic effect and quantum yield of photocatalytic induced reactions

From the previous experimental results, different contributions to the rate of formaldehyde formation have been calculated. On one hand, when single ozonation experiments were carried out at pH=3, the contribution of O_3 indirect reactions (r_{OH-O3}) can be neglected and

therefore, the observed reaction rate at this pH would only be due to the direct ozone-methanol reaction (r_{O3}). This was extrapolated to photocatalytic ozonation considering the same contribution of ozone-methanol direct reaction than in the absence of light. Additionally, for photocatalytic treatments, another contribution needs to be considered due to the photogenerated oxidizing species (i.e. h^+ and $^{\bullet}OH$ from reactions (1)-(6) and (15)) apart from the direct or indirect ozonation mechanism. This contribution, named r_{hv}, is the observed rate of CHOH formation in photocatalytic oxidation, and was calculated as the difference between the observed reaction rate r_{CHOH} and the direct-indirect ozone reactions in photocatalytic ozonation. On the other hand, when reactions were carried out at pH=7, the contribution of indirect ozone reactions become very important. In this case, this contribution was calculated by subtracting the ozone-direct reaction rate (calculated at pH=3 at the same operating conditions) to the observed reaction rate of formaldehyde formation during single ozonation experiments. Also, these results were extrapolated to photocatalytic ozonation at pH=7. The different contributions to the global reaction rate of formaldehyde formation during methanol oxidation have been summarized in Table 2. Regarding the photocatalytic contribution, it is noticeable the increase underwent in the light induced reaction rate when ozone was present compared to the one of photocatalytic oxidation at the same operating conditions. The degree of enhancement produced as a consequence of O_3 was calculated as follows:

$$E = \frac{r_{hv}(TiO_2/O_3/UVA) - r_{hv}(TiO_2/O_2/UVA)}{r_{hv}(TiO_2/O_2/UVA)} \cdot 100 \quad (\%) \qquad (22)$$

Table 2 shows the values obtained for all the photocatalytic ozonation experiments. The enhancement observed in the photocatalytic contribution increased from ca 53% to 57% when increasing ozone concentration in the feeding effluent at pH=3, although slight differences were observed when using 20 or 30 mgL^{-1} O_3 as commented in the previous section. The highest enhancement was observed at pH=7 with 30 mgL^{-1} of ozone. This parameter can be considered as a real evidence of the synergism produced between ozone and irradiated TiO_2.

At the experimental conditions used (high excess of CH_3OH), the reaction rate calculated for the photocatalytic contribution (r_{hv}) can be well considered as the reaction rate of oxidizing species formation due to light induced reactions. Therefore, the quantum yield of these reactions (light induced ones) can be calculated taking into account the absorbed light intensity at the operating conditions used (see Table 1). The calculated quantum yields of (ϕ_{hv}) for photocatalytic oxidation and photocatalytic ozonation processes are presented in Table 2. The quantum yield of photogenerated species formation in photocatalytic ozonation at pH=3 was found to be increased twice and near triple times the value observed for

photocatalytic oxidation as ozone concentration increased. Quantum yield reached a plateau at high ozone concentrations, as can also be observed in Fig. 7 where the evolution of the quantum yield with ozone concentration has been depicted. This trend suggests that a limiting reaction rate has been reached in the system due to the reaction of hydroxyl radicals with O_3. Sun and Bolton [21] also observed this behavior while studying the photocatalytic oxidation of methanol with the addition of hydrogen peroxide as an electron acceptor. On the other hand, the highest improvement of the quantum yield has been observed in the experiment of photocatalytic ozonation at pH=7 reaching a value near 3 photogenerated oxidizing species per absorbed photon.

The maximum quantum yield of formaldehyde formation expected during photocatalytic oxidation is $\phi_{CHOH,\max} = \phi_{h\nu,\max}$ =1.5 mol·einstein^{-1}, according to the reaction mechanism proposed where 2 photons are needed to produce 3 oxidizing species (i.e. holes and/or hydroxyl radicals) taking into account also the radical $O_2^{\bullet-}/HO_2^{\bullet}$ formed from CH_3OH oxidation [6]. This maximum becomes even greater ($\phi_{h\nu,\max-O3}$ =2-3) when ozone is present depending on pH, due to reactions (13)-(15) where ozone needs 1 e^- per $^{\bullet}OH$ formed, and the generation of H_2O_2 from direct methanol ozonation (reaction (20)), that acts as an electron acceptor (reaction (6)) needs also 1 e^- per $^{\bullet}OH$ formed. The maximum quantum yield at basic-neutral pH when O_3 is present has not been accurately calculated since ozone-indirect reactions are closely related to the reactions involving photogenerated species. Thus, the calculated values seem to be reasonable although they should be taken with caution, especially that calculated at pH=7 where the contribution of the indirect-ozone reaction has been taken as the same than in single ozonation and may be underestimated. Further work will be carried out to quantitatively calculate the different contributions through a detailed reaction mechanism for the AOPs studied (photocatalytic oxidation, ozonation and photocatalytic ozonation). Despite this it is clear that ozone exerts a positive effect on the photocatalytic induced reactions (not only O_3 direct and indirect reactions) due to two main factors: (i) ozone acts as an electron acceptor, (ii) hydrogen peroxide usually formed during direct ozonation reactions also acts as an electron acceptor, both leading to higher amount of hydroxyl radicals per photon absorbed and also reducing the recombination process to some extent.

3.2.4. Simplified economic considerations

In addition to the benefits observed with the combined treatment, i.e. photocatalytic ozonation (TiO_2/O_3/UVA), in the reaction rate of formaldehyde formation, the synergistic effect between ozone and irradiated TiO_2 and the highest quantum yield of photo-generated

oxidizing species production, one important issue in the application of combined treatments is the economy of the process. Accordingly, to compare the different systems, costs associated with the normal operation have been evaluated by taking into account the oxygen and electrical energy consumed to generate the oxidants and/or radiation and the amount of formaldehyde formed. It has to be highlighted that this simplified economic study aims only the comparison of the systems (i.e. investments, loss of TiO_2 activity and separation, and other factors are not considered) not providing an actual costs estimation.

According to Rivas et al. (2009) [45] for the same ozone generator, the dependence between O_3 production and current consumption can be estimated as:

$$O_3(\%\ of\ \max.\ flow\ rate\ in\ g{\cdot}L^{-1}) = 186{\cdot}current\ consumption\ in\ A \quad (23)$$

with maximum mass flow rate from oxygen 12 gh^{-1}. From the experimental conditions for 10 and 30 mgL^{-1} O_3 at 30 Lh^{-1} those are 2.5 and 7.5 % of the maximum amount produced, respectively. In photocatalytic experiments it is also necessary to take into account the lamps energy consumption (2 lamps with an input power of 15 W). The cost associated with electricity has been considered 0.14 €$(kWh)^{-1}$ according to the local supplier. In addition, in all the experiments oxygen from cylinders was used which has a cost of 0.262 €h^{-1} [45] at a flow rate of 30 Lh^{-1}.

With the above data, Table 3 shows the results obtained to produce 0.001 mol of formaldehyde from methanol oxidation taking into account the time needed. It can be observed that the main contribution (of the considered) is the oxygen consumption. It has to be pointed out that this contribution would be far different if air from atmosphere was used both in photocatalytic oxidation and ozonation runs (in the latter two using an air compressor) since there are ozone generators able to work with air. The operation costs (as calculated here) are always higher in photocatalytic experiments or ozonation alone than in the combined process, especially when working at pH=7, where the reaction time is highly reduced. Therefore, photocatalytic ozonation treatment is not only attractive from the point of view of their performance in terms of reaction rates but also in terms of economic considerations, where the synergism between ozone and TiO_2 photocatalysis is also clear. However, it has to be emphasized that this simplified economic study could give different results in every particular case taking into account the necessities of effluent mineralization; discharge limits required; investment and replacement costs, etc. as reported before [45] where ozone treatments involved higher costs at the same mineralization degree obtained.

Conclusions

Major conclusions reached in this study are:

- Absorbed light intensity during photocatalytic oxidation of methanol was indirectly calculated at different pH values and was always higher than 90% of that impinging the reactor for the catalyst loading used (0.5 gL^{-1} of TiO_2 P25).
- The presence of ozone during photocatalytic ozonation at pH=3 exerts a positive effect on the reaction rate of formaldehyde formation respect to photocatalytic oxidation. This was not only due to the direct ozone-methanol reaction, but also due to the reaction of dissolved ozone and hydrogen peroxide (formed upon CH_3OH ozonation), electron acceptors to produce higher concentration of hydroxyl radicals.
- An increase in ozone concentration exert a positive but low effect during photocatalytic ozonation likely due to self-scavenging reactions between $^{\bullet}OH$ and ozone or hydrogen peroxide.
- The quantum yield calculated for photo-generated oxidizing species during photocatalytic oxidation at pH=3 was $\phi_{h\nu}$=0.34 mol·einstein^{-1}. This parameter was increased to around $\phi_{h\nu}$=0.80 mol·einstein^{-1} when combining TiO_2/O_3/UVA. This enhancement was even higher at pH=7 from $\phi_{h\nu}$=0.29 to $\phi_{h\nu}$=3.27 mol·einstein^{-1}. Therefore, a clear synergism between ozone and black light photocatalytic oxidation with TiO_2 is pointed out due to the decrease of the recombination process. The reaction of dissolved ozone and hydrogen peroxide with photo-generated electrons is likely the reason of the reaction rate enhancement.
- Simplified economic evaluation taking into account only normal operation has shown that photocatalytic ozonation could be a cost-effective treatment depending on the actual necessities of the effluent to be treated.

Acknowledgements

This work has been supported by the Spanish Ministerio de Ciencia e Innovación (MICINN) and European Feder Funds through the project CTQ2009-13459-C05-05/PPQ. A. Rey thanks the University of Extremadura for a post-doctoral research contract.

References

[1] K. Kabra, R. Chaudhary, R. L. Sawhney. Treatment of hazardous organic and inorganic compounds through aqueous-phase photocatalysis: A review. Ind. Eng. Chem. Res. 43 (2004) 7683-7696.

[2] S. Malato, P. Fernández-Ibáñez, M.I. Maldonado, J. Blanco, W. Gernjak. Decontamination and disinfection of water by solar photocatalysis: Recent overview and trends. Catal. Today 147 (2009) 1–59.

[3] M. N. Chong, B. Jin, C. W. K. Chow, C. Saint. Recent developments in photocatalytic water treatment technology: A review. Water Res. 44 (2010) 2997-3027.

[4] C. Adán, A. Bahamonde, M. Fernández-García, A. Martínez-Arias. Structure and activity of nanosized iron-doped anatase TiO2 catalysts for phenol photocatalytic degradation. Appl. Catal. B: Environ. 72 (2007) 11–17

[5] T. E. Agustina, H. M. Ang, V. K. Vareek. A review of synergistic effect of photocatalysis and ozonation on wastewater treatment. J. Photochem. Photobiol. C: Photochem. Rev. 6 (2005) 264-273.

[6] V. Augugliaro, M. Litter, L. Palmisano, J. Soria. The combination of heterogeneous photocatalysis with chemical and physical operations: A tool for improving the photoprocess performance. J. Photochem. Photobiol. C Photochem. Rev. 7 (2006) 127.

[7] P. Salvador. On the nature of photogenerated radical species active in the oxidative degradation of dissolved pollutants with TiO2 aqueous suspensions: A revision in the light of the electronic structure of adsorbed water. J. Phys. Chem. C 111 (2007) 17038-17043.

[8] M. A. Henderson. A surface perspective on TiO2 photocatalysis. Surface Sci. Reports 66 (2011) 185-297.

[9] S. Goldstein, D. Behar, J. Rabani. Mechanism of visible light photocatalytic oxidation of methanol in aerated aqueous suspensions of carbon-doped TiO2. J. Phys. Chem. C. 112 (2008) 15134-15139.

[10] S. Goldstein, D. Behar, J. Rabani. Nature of the oxidizing species formed upon UV photolysis of C-TiO2 aqueous suspensions.

[11] F. J. Beltran. Ozone reaction kinetics for water and wastewater systems. Boca Raton, CRC Press, 2004, Florida (USA).

[12] M. Mvula, C. von Sonntag. Ozonolysis of Phenols in Aqueous Solution. Org. Biomol. Chem. 1 (2003) 1749-1756.

[13] A. Leitzke, C. von Sonntag. Ozonolysis of Unsaturated Acids in Aqueous Solution: Acrylic, Methacrylic, Maleic, Fumaric and Muconic Acids. Ozone Sci. Eng. 31 (2009) 301-308.

[14] S. Rakowski, D. Cherneva. Kinetics and mechanism of the reaction of ozone with aliphatic alcohols. Int. J. Chem. Kinetics 22 (1990) 321-329.

[15] R. Rajeswari, S. Kanmani. Degradation of Pesticide by Photocatalytic Ozonation Process and Study of Synergistic Effect by Comparison with Photocatalysis and UV/Ozonation Processes. J. Adv. Oxid. Technol. 12 (2009) 208-214.

[16] J. F. Garcia-Araya, F. J. Beltran, A. Aguinaco. Diclofenac removal from water by ozone and photolytic TiO2 catalysed processes. J. Chem. Technol. Biotechnol. 85 (2010) 798-804.

[17] L. D. Zou, B. Zhu. The synergistic effect of ozonation and photocatalysis on color removal from reused water. J. Photochem. Photobiol. A Chem. 196 (2008) 24-32.

[18] F. J. Beltran, F. J. Rivas, O. Gimeno, M. Carbajo. Photocatalytic enhanced oxidation of fluorene in water with ozone. Comparison with other chemical oxidation methods. Ind. Eng. Chem. Res. 44 (2005) 3419-3425.

[19] F. J. Beltran, A. Aguinaco, J. F. Garcia-Araya. Mechanism and kinetics of sulfamethoxazole photocatalytic ozonation in water. Water Res. 43 (2009) 1359-1369.

[20] G.V. Buxton, C.L. Greenstock, W.P. Helman, A.B. Ross. Critical review of rate constants for reactions of hydrated electrons, hydrogen atoms and hydroxyl radicals (·OH/·O-) in aqueous solution. J. Phys. Chem. Ref. Data 17 (1988) 513-886.

[21] L. Sun, J. R. Bolton. Determination of the quantum yield for the photochemical generation of hydroxyl radicals in TiO2 suspensions. J. Phys. Chem. 100 (1996) 4127-4134.

[22] T. Tachikawa, S. Tojo, K. Kawai, M. Endo, M. Fujitsuka, T. Ohno, K. Nishijima, Z. Miyamoto, T. Majima. Photocatalytic oxidation reactivity of holes in the sulfur- and carbon-doped TiO2 powders studied by time-resolved diffuse reflectance spectroscopy. J. Phys. Chem B 108 (2004) 19299-19306.

[23] C. Wang, J. Rabani, D. W. Bahnemann, J. K. Dohrmann. Photonic efficiency and quantum yield of formaldehyde formation from methanol in the presence of various TiO2 photocatalysts. J. Photochem. Photobiol. A Chem. 148 (2002) 169-176.

[24] R. Gao, J. Stark, D. W. Bahnemann, J. Rabani. Quantum yields of hydroxyl radicals in illuminated TiO2 nanocrystallite layers. J. Photochem. Photobiol. A Chem. 148 (2002) 387-391.

[25] J. Marugan, D. Hufschmidt, M. J. Lopez-Muñoz, V. Selzer, D. Bahnemann. Photonic efficiency for methanol photooxidation and hydroxyl radical generation on silica-supported TiO2 photocatalysts. Appl. Catal. B Environ. 62 (2006) 201-207.

[26] J. Hoigné, H. Bader. Rate constant of reactions of ozone with organic and inorganic compounds in water I. Non-dissociating organic compounds. Water Res. 17 (1983) 173-183.

[27] T. Nash. The colorimetric estimation of formaldehyde by means of the Hantzsch reaction. Biochemistry 55 (1953) 416-421.

[28] R. Flyunt, A. Leitzke, G. Mark, E. Mvula, E. Reisz, R. Schick, C. von Sonntag. Determination of ·OH, O2·-, and hydroperoxide yields in ozone reactions in aqueous solution. J. Phys. Chem. B 107 (2003) 7242-7253.

[29] W. Masschelein, M. Denis, R. Ledent. Spectrophotometric determination of residual hydrogen peroxide. Water Manag. Water Sewage Works, August (1977) 69-72

[30] H. Bader, J. Hoigné. Determination of ozone in water by the indigo method. Water Res. 15 (1981) 449-456.

[31] C. G. Hatchard, C. A. Parker. A new sensitive chemical actinometer. 2. Potassium ferrioxalate as a standard chemical actinometer. Proceed. Of the Royal Society of London Series A. Mathematical and Physical Sciences 235 (1956) 518.

[32] E. B. Sandell. Colorimetric determination of traces of metals. Interscience Pubs., New York (1959).

[33] N. Serpone, A. Salinaro. Terminology, Relative Photonic Efficiencies and Quantum Yields in Heterogeneous Photocatalysis. Part I: Suggested Protocol. Pure Appl. Chem. 71 (1999) 303-320.

[34] O. M. Alfano, M.I. Cabrera, A.E. Cassano. Photocatalytic reactions involving hydroxyl radical attack-I. Reaction kinetics formulation with explicit photon absorption effects. J. Catal. 172 (1997) 370-379.

[35] M.I. Cabrera, A.C. Negro, O.M. Alfano, A.E. Cassano. Photocatalytic reactions involving hydroxyl radical attack-II. Kinetics of the decomposition of trichloroethylene using titanium dioxide. J. Catal. 172 (1997) 380-390.

[36] R.J. Brandi, O.M. Alfano, A.E. Cassano. Rigorous model and experimental verification of the radiation field in a flat-plate solar collector simulator employed for photocatalytic reactions. Chem. Eng. Sci. 54 (1999) 2817-2827.

[37] A. Brucato, A. E. Cassano, F. Grisafi, G. Montante. L. Rizzuti, G. Vella. Estimating radiant fields in flat heterogeneous photoreactors by the six-flux model. AIChE J. 52 (2006) 3882-3890.

[38] B. Toepfer, A. Gora, G. Li Puma. Photocatalytic oxidation of multicomponent solutions of herbicides: Reaction kinetics analysis with explicit photon absorption effects. Appl. Catal. B Environ. 68 (2006) 171-180.

[39] V. Loddo, M. Addamo, V. Augugliaro, L. Palmisano, M. Schiavello, E. Garrone. Optical properties and quantum yield determination in photocatalytic suspensions. AIChE J. 52 (2006) 2565-2574.

[40] H.Y. Chen, O. Zahraa, M. Bouchy. Inhibition of the adsorption and photocatalytic degradation of an organic contaminant in an aqueous suspension of TiO2 by inorganic ions. J. Photochem. Photobiol. A 108 (1997) 37-44.

[41] P.A. Connor, A. J. McQuillan, Phosphate adsorption onto TiO2 from aqueous solutions: An in situ internal reflection Infrared Spectroscopic study. Langmuir 15 (1999) 2916-2921.

[42] Y. Du, J. Rabani. The measure of TiO2 photocatalytic efficiency and the comparison of different photocatalytic titania. J. Phys. Chem. B 107 (2003) 11970-11978.

[43] G. Lefevre. In situ Fourier-transform infrared spectroscopy studies of inorganic ions adsorption on metal oxides and hydroxides. Adv. Colloid Interf. Sci. 107 (2004) 109-123.

[44] S. Rakovski, D. Cherneva. Kinetics and mechanism of the reaction of ozone with aliphatic alcohols. Int. J. Chem. Kinetics 22 (1990) 321-329.

[45] F.J. Rivas, A. Encinas, B. Acedo, F.J. Beltrán. Mineralization of bisphenol A by advanced oxidation processes. J. Chem. Technol. Biotechnol. 84 (2009) 589-594.

Table(s)

Table 1. Rate and photonic efficiency of CHOH formation and absorbed and fraction light intensity

C_{TiO2} ($g \cdot L^{-1}$)	pH_0	r_{CHOH}/r_{CO2} ($M \cdot min^{-1}$)	ξ ($mol \cdot einstein^{-1}$)	I_a ($einstein \cdot L^{-1} \cdot min^{-1}$)	F_s
0.025	7	6.05×10^{-6}	0.23	1.27×10^{-5}	0.47
0.05	7	8.29×10^{-6}	0.31	1.73×10^{-5}	0.65
0.1	7	1.07×10^{-5}	0.40	2.24×10^{-5}	0.84
0.3	7	1.16×10^{-5}	0.44	2.43×10^{-5}	0.91
0.5	7	1.22×10^{-5}	0.46	2.55×10^{-5}	0.96
1	7	1.23×10^{-5}	0.46	2.57×10^{-5}	0.97
2	7	1.34×10^{-5}	0.50	2.80×10^{-5}	~1.0
3	7	1.17×10^{-5}	0.44	2.45×10^{-5}	0.92
0.5	7[a]	7.51×10^{-6}	0.28	2.55×10^{-5}	0.96
0.025	3	2.65×10^{-6}	0.10	7.81×10^{-6}	0.29
0.05	3	4.01×10^{-6}	0.15	1.18×10^{-5}	0.44
0.1	3	4.62×10^{-6}	0.20	1.56×10^{-5}	0.59
0.5	3	8.77×10^{-6}	0.33	2.60×10^{-5}	0.97
1	3	8.82×10^{-6}	0.33	2.61×10^{-5}	0.98
0.5	3[b]	6.76×10^{-6}	0.26	2.60×10^{-5}	0.97

[a]Buffered solution (H_3PO_4 30 mM), [b]Experiment with HCOOH (10 mM)

Table 2. Experimental conditions, reaction rate contributions and quantum yield of the photocatalytic reactions

Process	Irradiation	C_{TiO2} ($g \cdot L^{-1}$)	$C_{O3,g\ inlet}$ ($mg \cdot L^{-1}$)	pH	r_{CHOH} ($M \cdot min^{-1}$)	r_{O3} [b] ($M \cdot min^{-1}$)	r_{OH-O3} [c] ($M \cdot min^{-1}$)	r_{hv} [d] ($M \cdot min^{-1}$)	E_{hv} (%)	ϕ_{hv} ($mol \cdot ein^{-1}$)
Photocatalytic oxidation (TiO_2/O_2/UVA)	on	0.5	0	3	8.77×10^{-6}	---	---	8.77×10^{-6}	0	0.34
	on	0.5	0	7	1.22×10^{-5}	---	---	1.22×10^{-5}	0	0.48
	on	0.5	0	7[a]	7.51×10^{-6}	---	---	7.51×10^{-6}	0	0.29
Ozonation (O_3)	off	0	10	3	1.02×10^{-5}	1.02×10^{-5}	0	---	---	---
	off	0	20	3	1.55×10^{-5}	1.55×10^{-5}	0	---	---	---
	off	0	30	3	1.97×10^{-5}	1.97×10^{-5}	0	---	---	---
	off	0	30	7[a]	1.55×10^{-4}	1.97×10^{-5}	1.35×10^{-4}	---	---	---
Photocatalytic ozonation (TiO_2/O_3/UVA)	on	0.5	10	3	2.91×10^{-5}	1.02×10^{-5}	0	1.89×10^{-5}	53	0.73
	on	0.5	20	3	3.63×10^{-5}	1.55×10^{-5}	0	2.08×10^{-5}	57	0.80
	on	0.5	30	3	3.91×10^{-5}	1.97×10^{-5}	0	1.94×10^{-5}	55	0.75
	on	0.5	30	7[a]	2.38×10^{-4}	1.97×10^{-5}	1.35×10^{-4}	8.36×10^{-5}	91	3.27

[a]Buffered solution (H_3PO_4 30 mM), [b]It coincides with r_{CHOH} for single ozonation experiments at pH=3, [c]Calculated from ozonation experiments by means of the difference between r_{CHOH}-r_{O3}, [d]Calculated by means of the difference between r_{CHOH}-r_{O3}-r_{OH-O3}

Table 3. Estimated costs for the transformation of 10^{-3} mol CH_3OH (CHOH formed)

Process	pH	$C_{O3g\ inlet}$ ($mg \cdot L^{-1}$)	Time used (h)	E_{O3} (kWh)	E_{UVA} (kWh)	Electricity (€)	O_2 (€)	Cost/mmol converted ($€ \cdot mmol^{-1}$)
Photocatalytic oxidation (TiO_2/O_2/UVA)	3	0	1.90	0	5.70×10^{-2}	7.98×10^{-3}	4.97×10^{-1}	5.05×10^{-1}
	7	0	2.22	0	6.66×10^{-2}	9.32×10^{-3}	5.81×10^{-1}	5.90×10^{-1}
Ozonation (O_3)	3	10	1.63	4.83×10^{-3}	0	6.76×10^{-4}	4.27×10^{-1}	4.28×10^{-1}
	7	30	0.11	9.54×10^{-4}	0	1.34×10^{-4}	2.80×10^{-2}	2.80×10^{-2}
Photocatalytic ozonation (TiO_2/O_3/UVA)	3	10	0.57	1.69×10^{-3}	1.72×10^{-2}	2.64×10^{-3}	1.50×10^{-1}	1.52×10^{-1}
	7	30	0.07	6.21×10^{-4}	2.10×10^{-3}	3.81×10^{-4}	1.80×10^{-2}	1.90×10^{-2}

Figure(s)

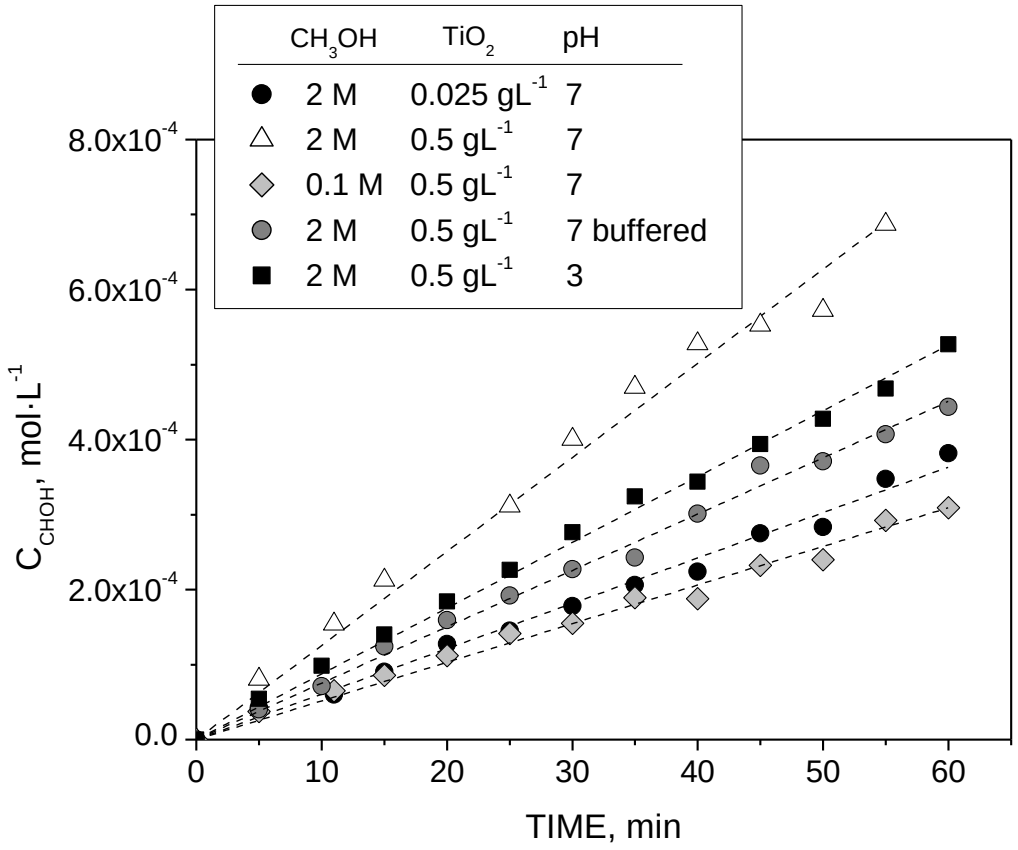

Figure 1. Time-evolution of formaldehyde formation during methanol photocatalytic oxidation experiments. Conditions: T=25º C, Q_g=30 L·h^{-1} (O_2)

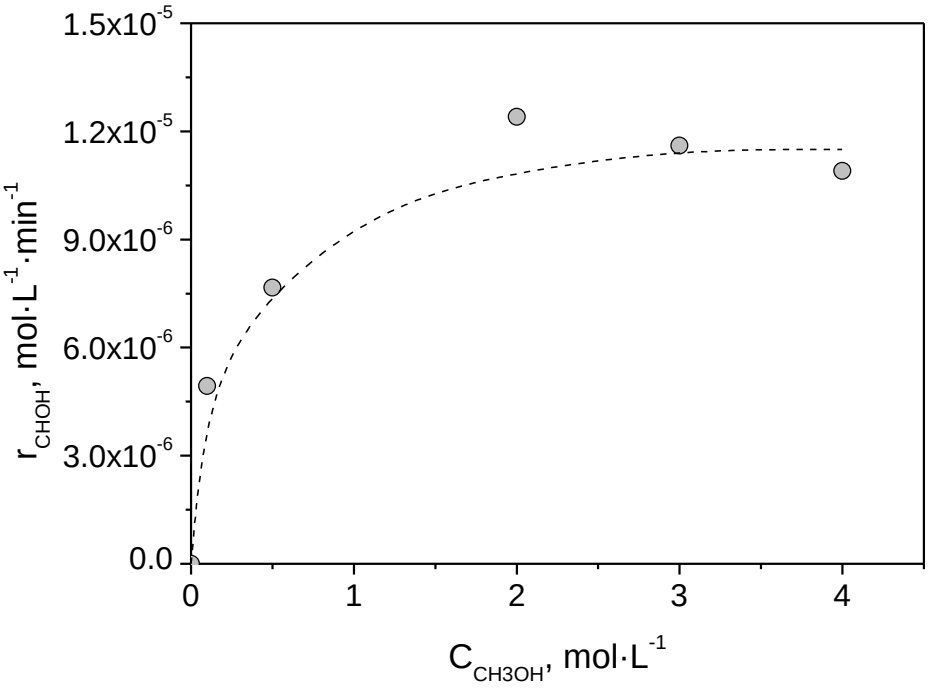

Figure 2. Rate of formaldehyde formation vs. methanol concentration in photocatalytic oxidation experiments. Conditions: pH=7, T=25º C, C_{TiO2}=2 g·L^{-1}, Q_g=30 L·h^{-1} (O_2 or O_3/O_2)

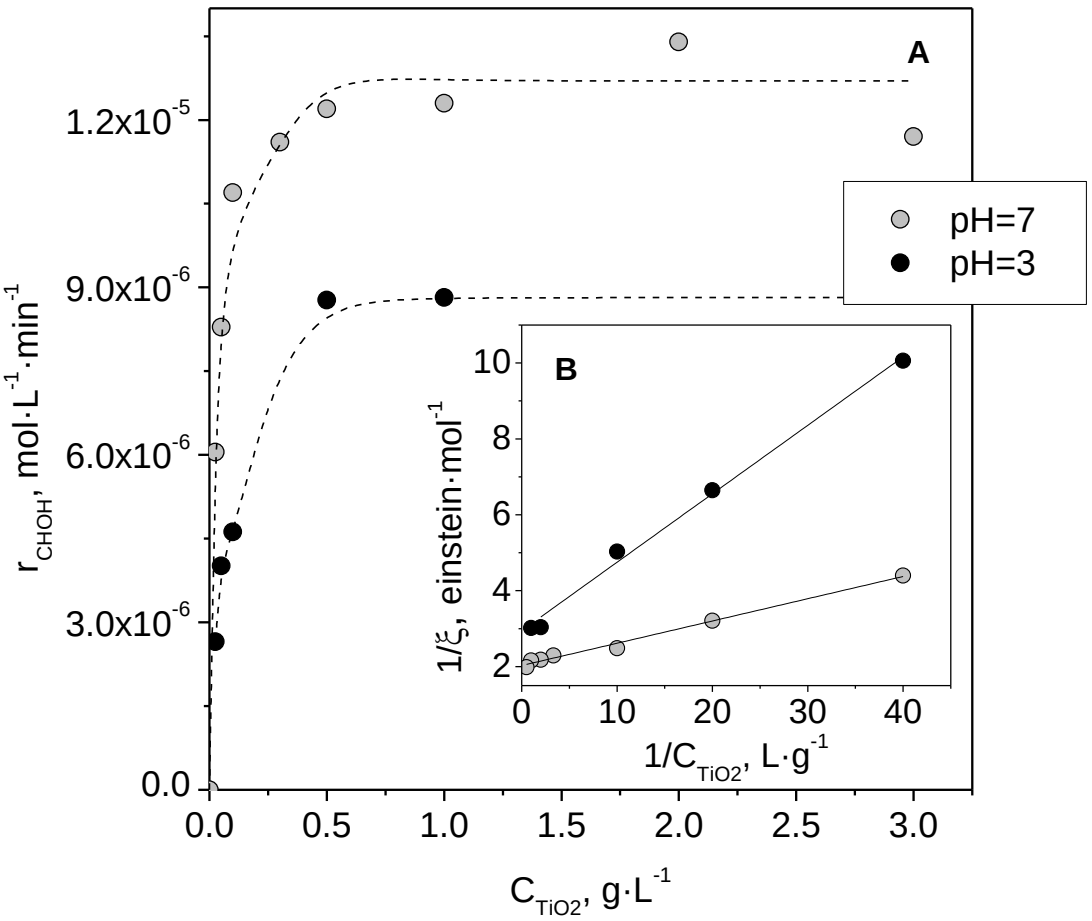

Figure 3. (A): Rate of formaldehyde formation vs. TiO_2 loading in methanol photocatalytic oxidation experiments. (B): Fitting results of linearized eq.(19). Conditions: pH=7 and 3, T=25º C, Q_g=30 $L \cdot h^{-1}$ (O_2 or O_3/O_2).

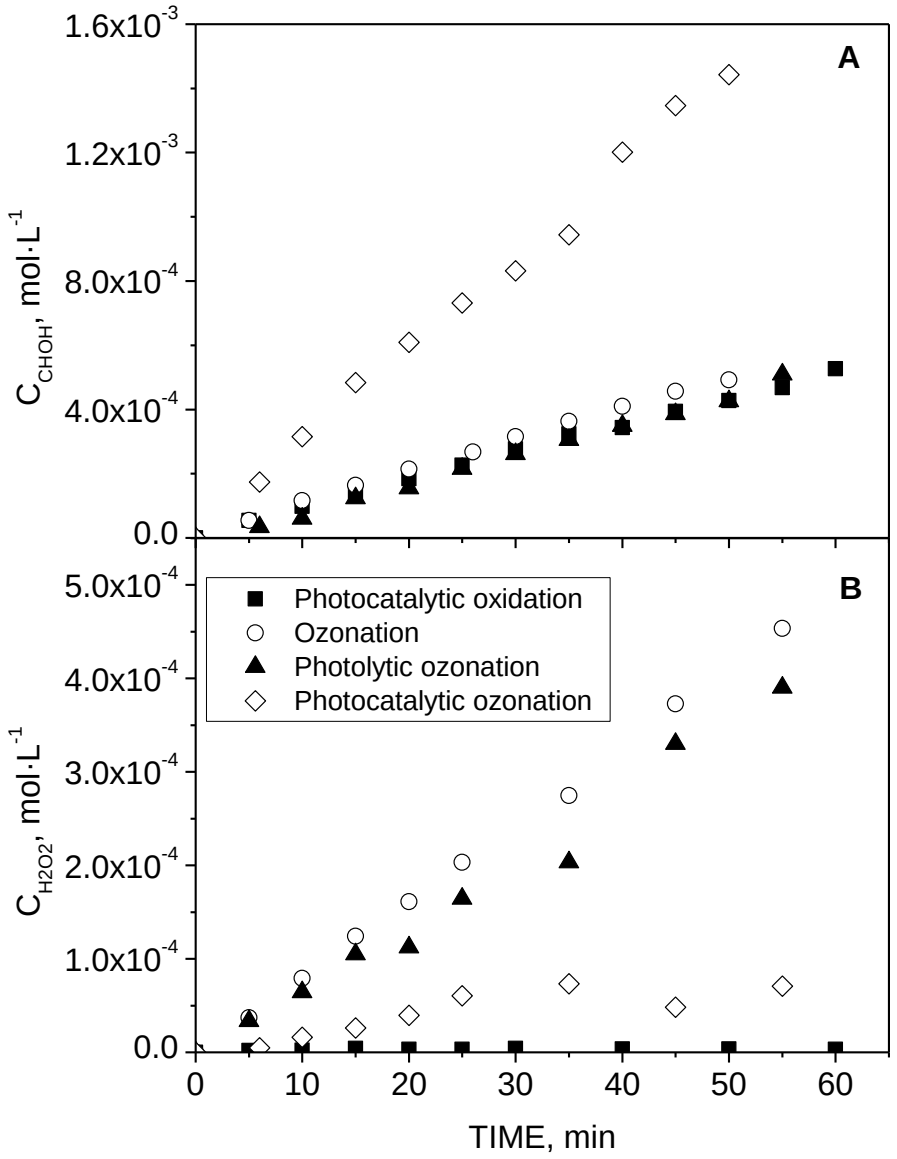

Figure 4. Time-evolution of formaldehyde (A) and hydrogen peroxide (B) concentrations during ozonation and photocatalytic oxidation/ozonation experiments. Conditions: pH=3, T=25º C, C_{TiO2}=0.5 g·L^{-1}, $C_{O3g\ inlet}$=10 mg·L^{-1}, Q_g=30 L·h^{-1} (O_2 or O_3/O_2)

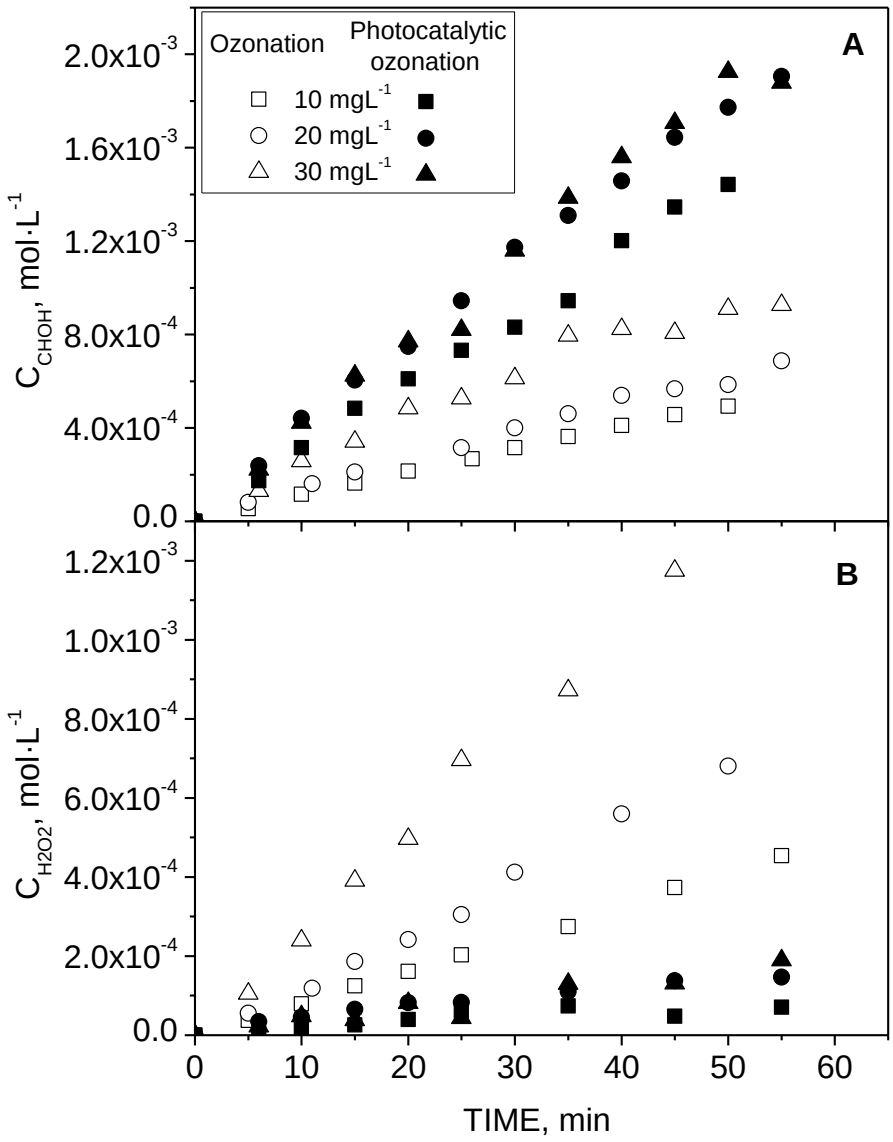

Figure 5. Time-evolution of formaldehyde (A) and hydrogen peroxide (B) concentrations during methanol ozonation and photocatalytic ozonation experiments. Conditions: pH=3, T=25º C, C_{TiO2}=0.5 g·L^{-1}, $C_{O3g\ inlet}$=10, 20, 30 mg·L^{-1}, Q_g=30 L·h^{-1} (O_3/O_2)

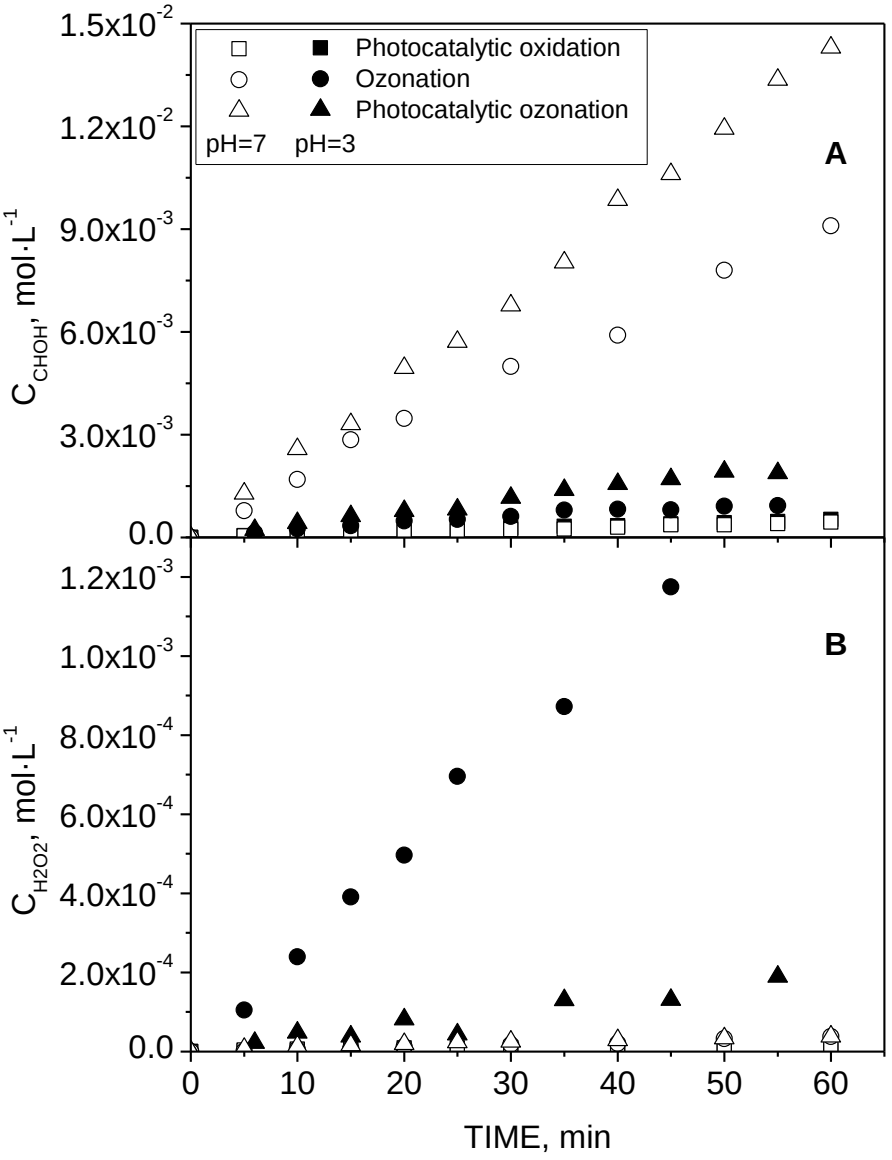

Figure 6. Time-evolution of formaldehyde (A) and hydrogen peroxide (B) concentrations during methanol ozonation and photocatalytic oxidation/ozonation experiments. Conditions: pH=3, 7, T=25º C, C_{TiO2}=0.5 g·L^{-1}, $C_{O3g\ inlet}$= 30 mg·L^{-1}, Q_g=30 L·h^{-1} (O_2 or O_3/O_2)

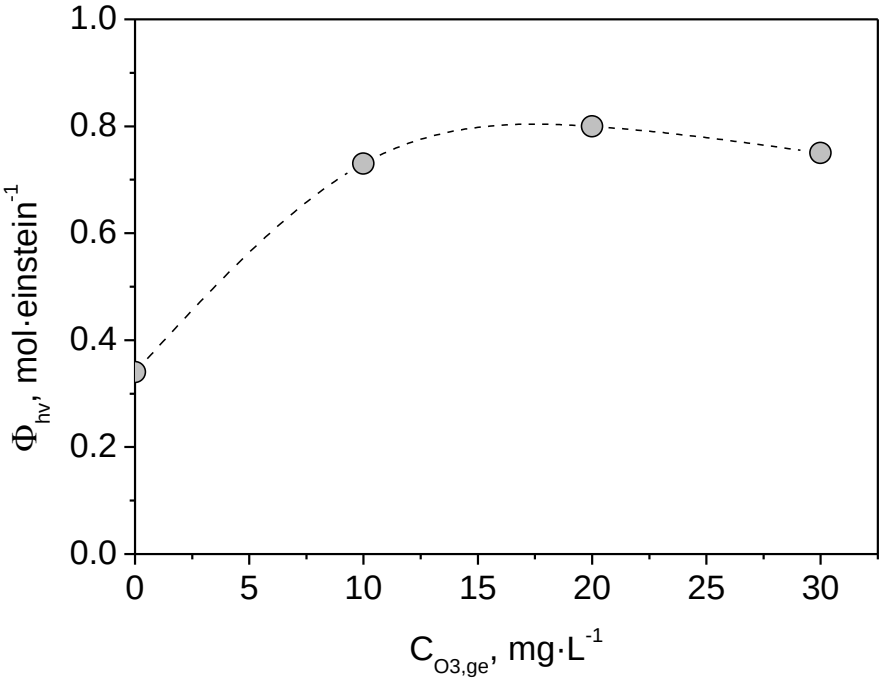

Figure 7. Evolution of quantum yield of oxidizing species formation through light induced reactions with ozone inlet concentration. Conditions: pH=3, T=25º C, C_{TiO2}=0.5 g·L^{-1}, Q_g=30 L·h^{-1} (O_2 or O_3/O_2)